ACR No. L4H17

NATIONAL ADVISORY COMMITTEE FOR AERONAUTICS

WARTIME REPORT

ORIGINALLY ISSUED
October 1944 as
Advance Confidential Report L4H17

VARIATION OF PEAK PITCHING-MOMENT COEFFICIENTS FOR SIX AIRFOILS AS AFFECTED BY COMPRESSIBILITY

By Harold E. Cleary

Langley Memorial Aeronautical Laboratory
Langley Field, Va.

NACA

WASHINGTON

NATIONAL ADVISORY COMMITTEE FOR AERONAUTICS

ADVANCE CONFIDENTIAL REPORT

VARIATION OF PEAK PITCHING-MOMENT COEFFICIENTS FOR SIX AIRFOILS AS AFFECTED BY COMPRESSIBILITY

By Harold E. Cleary

SUMMARY

Pressure-distribution tests of six NACA 16-series propeller sections with 1-foot chords were conducted in the NACA 8-foot high-speed tunnel to determine the compressibility effects on peak section pitching-moment coefficients. The data are presented as curves of peak section pitching-moment coefficient against Mach number, thickness ratio, and camber.

The peak pitching-moment coefficients were found to occur in the regions of positive and negative stall. For these conditions, especially for the thicker airfoils and in the region of positive stall, the critical speed occurred at Mach numbers as low as 0.30 and marked changes of the peak moment coefficient occurred at Mach numbers as low as 0.53. Increases in thickness and camber were found to accentuate the compressibility effects on peak moment coefficient.

INTRODUCTION

The problem of the excessive twisting moments developed by propeller blades and the consequent failure of pitch-control mechanisms have aroused interest in the factors contributing to these twisting moments. One of these factors is the aerodynamic pitching moment of the propeller-blade sections.

The conditions encountered on the blades for normal propeller operation are bracketed between positive and negative stall. The condition of positive stall is associated with take-off, climb, and pull-out; and negative stall might be associated with dive and dive entry.

The general effect of compressibility on the pitching-moment coefficient is shown in references 1 to 3, but the range of angle of attack tested is not sufficient to include the conditions for maximum moments. Some moment data are available for sections designed to delay adverse compressibility effects (reference 4), but again these data are limited to conditions below the points where the maximum values, both positive and negative, of the moment coefficient are reached. Further limitations of the tests of reference 4 are that the Reynolds numbers are lower than for the present tests and the tunnel-wall effects resulting from the larger ratio of model size to tunnel size are larger. Because of the importance of compressibility effects on airfoil characteristics, a detailed investigation of these effects is being conducted by the NACA. The present report includes a part of the data obtained from tests conducted in the NACA 8-foot high-speed tunnel on several airfoils covering representative ranges of thickness and camber. The data obtained in the present investigation constitute an extension of the results of reference 4, and part of the data were obtained to study the effects of the differences in the test conditions previously noted.

Use of 1-foot-chord models gave practically full-scale Reynolds numbers and reduced tunnel-wall effects. Use of pressure-distribution measurements in the central spanwise region of the models, which spanned the tunnel, gave practically two-dimensional results. Particular emphasis was placed on pressure-distribution tests rather than force tests because the type of phenomenon that occurs is more clearly illustrated. The Mach number range extended from 0.12 to 0.68.

APPARATUS AND METHODS

The NACA 8-foot high-speed tunnel, in which the tests were carried out, is a single-return circular-section closed-throat tunnel. The airspeed is continuously controllable from about 75 to 550 miles per hour. The turbulence of the air stream, as indicated by transition measurements on airfoils, is unusually low but somewhat higher than that of free air.

Six models having NACA 16-209, 16-509, 16-709, 16-215, 16-515, and 16-715 airfoil sections of 1-foot chord were

investigated. Thirty pressure orifices distributed along the chord were located at practically the same spanwise station at the center of the air stream. The airfoil profiles and orifice locations are shown in figure 1. The airfoil ordinates were calculated by the method described in reference 4.

The model, when mounted in the tunnel, completely spanned the jet (fig. 2). Except for auxiliary streamline-wire bracing, required by structural considerations, the standard NACA 8-foot high-speed tunnel mounting and setup were employed. Tests at low and medium speeds with and without braces indicated that interference of the auxiliary supports on the flow at the measurement station was negligible.

Measurements were made, for the most part, of the chordwise pressure distribution at the midspan region. The surface orifices in the airfoil were connected to a multiple-tube manometer located outside the test section. The pressure tubing connecting the orifices was of small diameter and was located within the wing. Simultaneous recordings of the pressures at all orifices in the wing were made by photographing the multiple-tube manometer.

The Mach number range extended from 0.12 to 0.68. The Reynolds number range of the tests and the variation of the Reynolds number with Mach number are shown in figure 3.

RESULTS

The data presented in this report are in the form of dimensionless coefficients.

α angle of attack, degrees

M Mach number

c_l section lift coefficient

c_m section pitching-moment coefficient

P pressure coefficient $\left(\frac{\text{Local static pressure - Free-stream static pressure}}{\frac{1}{2}\rho V^2}\right)$

t/c thickness-chord ratio

M_{cr} critical Mach number, defined as the value of free-stream Mach number at which a Mach number of 1.0 is first attained at any point in the flow field

R Reynolds number

Subscripts:

$c/4$ about quarter-chord axis

c.g. about center-of-gravity axis

max maximum

cr critical

Determination of the location of the center of gravity of a large number of this series of airfoils indicates that the general expression for center-of-gravity location of a homogeneous section is

$$x_{c.g.} = 0.484 \times \text{Chord}$$

$$y_{c.g.} = 0.0435 \times \text{Design lift coefficient} \times \text{Chord}$$

where $x_{c.g.}$ is distance behind the leading edge and $y_{c.g.}$ is distance above the chord.

A sample plot of the variation with angle of attack of the lift coefficient and the pitching-moment coefficients about the quarter-chord and center-of-gravity axes for the airfoil sections reported herein is given in figure 4. These data are for the NACA 16-509 airfoil at a Mach number of 0.33. The values of lift and moment coefficients were determined by integration of the normal-pressure distribution. Analysis has shown that up to the value of maximum lift coefficient the normal-force coefficient and the lift coefficient are essentially the same.

Peak values of moment coefficient for all the airfoils at all values of Mach number tested were determined from plots similar to figure 4. The values referred to as "peak moment coefficients" are those for which the slope of the moment variation with angle of attack is zero. Higher values may be obtained beyond the stall.

The moments taken about the quarter-chord point are of interest in wing design because this point has closely approximated the aerodynamic center of the older conventional airfoils. Consideration of the moments about the center-of-gravity axis enters into propeller design, for which the sections reported herein were primarily developed.

The variation of the peak section moment coefficients about the quarter-chord and center-of-gravity axes with Mach number is presented in figure 5. The scatter shown by some of these results is a consequence of the unsteady flow in the stalled region. The dash-line curves in figure 5 were obtained by multiplying the value of the moment coefficient at $M = 0.20$ by the Glauert-Ackeret relation $1/\sqrt{1 - M^2}$. This relation is not strictly applicable because the angle of attack is not constant and because the flow departs from potential flow in the stall region.

Pressure-distribution diagrams for the NACA 16-715 airfoil at an angle of attack of 8° for Mach numbers of 0.25, 0.53, and 0.64 are given in figure 6. These data illustrate the changes in chordwise pressure load distribution over the upper surface of the airfoil as affected by increase of Mach number. No important changes in the pressure distributions over the lower surface were found near the stall within the Mach number range tested.

Figure 7 is a comparison of the pressure distributions in the negative stall region at Mach numbers of 0.25 and 0.60 over the NACA 16-509 and 16-515 airfoil sections, which have the same design camber and different thickness.

In order to illustrate the variation of peak moment coefficient with thickness ratio, a cross plot of the data given in figures 5(a) and 5(b) for the two airfoils cambered to give $c_l = 0.2$ at an angle of attack of 0° is presented in figure 8 for three values of Mach number. In order to illustrate the effect of camber on the peak moment coefficient, a similar cross plot for the two thickness ratios tested is presented in figure 9.

A comparison of the pressure distributions of three differently cambered airfoils is presented in figure 10 for the NACA 16-209, 16-509, and 16-709 sections at an angle of attack of -6° and Mach numbers of 0.25 and 0.60.

These data, as presented, have not been corrected for wind-tunnel-wall interference. An analysis, however, has been made of these effects according to the methods of reference 5 which gave the following maximum corrections:

	Mach number	Lift	Moment coefficient	Drag coefficient	Angle of attack
Design lift range	Less than 1 percent	Less than -1 percent	-0.002	Less than 0.0001	Less than $\pm 0.01^\circ$
High lift range	1 percent	-2 percent	-0.002	0.001	$\pm 0.05^\circ$

The method of correction used has only qualitative application at high values of lift coefficient and supercritical values of Mach number. The corrections obtained, however, give a good estimate of the order of the interference effects.

DISCUSSION

Variation of Moment Coefficient with Angle of Attack

The variation of moment coefficient about the quarter-chord axis with angle of attack, as shown by the sample data of figure 4, indicates that the aerodynamic center is appreciably forward of the quarter-chord station. The peak values of moment coefficient are shown in this figure to occur in the region of positive and negative stall. The angles of attack at which the peak lift and moment coefficients occur (table I) are found, in general, to agree within 3° with a few scattered variations as high as 6° in the region of negative stall.

Variation of Peak Moment Coefficient with Mach Number

Subcritical region.- The comparison shown in figure 5 of the variation of moment coefficient with Mach number and the Glauert-Ackeret theoretical variation based on the moment coefficient at a Mach number of 0.20 shows close agreement with the data in most instances, and in

no case does the disagreement exceed a value of moment coefficient of 0.02. The theoretical variation is not applicable beyond the critical Mach number M_{cr}. The termination of the theoretical variations in figure 5 therefore indicates the critical Mach number for peak condition.

The higher values of critical Mach number obtained for the thinner of the airfoils tested are not in conformity with the theoretical results for this series of airfoils. At angles of attack considerably different from the design angle, the theoretical pressure distributions for the thinner airfoils indicate lower critical speeds than for the thicker airfoils, because the sharper leading edges of the thinner airfoils then cause higher superstream velocities. As a consequence of the steep pressure-recovery gradients associated with these superstream velocities, separation is believed to be induced which prevents the attainment of the superstream velocity indicated by theory. The separation phenomenon thus raises the critical speed of the thinner airfoils to appreciably higher values of Mach number than indicated by theory.

Supercritical region.- Relatively large, abrupt changes in the variation of peak moment coefficient with Mach number are found to occur in the stall regions for the thick highly cambered airfoil, as shown in figure 5(e) for the NACA 16-715 airfoil. The increments in moment coefficient are shown to be between 0.025 and 0.10.

For the thinner highly cambered NACA 16-709 airfoil, a similar abrupt change is shown in the curve for the moments taken about the center of gravity in the positive stall region, but no corresponding change in the moment taken about the quarter-chord axis is exhibited. This difference in moments taken about the two axes is a consequence of a change in the magnitude rather than in the distribution of the lift. No abrupt changes occur for the airfoils having lower camber in the range tested.

The fundamental pressure-distribution changes with Mach number that occur in conjunction with the changes in moment coefficient are shown in figure 6. The characteristic low-speed pressure distribution is shown for a Mach number of 0.25. At a Mach number of 0.53, local supersonic flow has been attained over the leading edge.

This condition gives rise to incipient shock and it may be noted that, although the pressure distribution is changing, the change is still slight. Further increase in Mach number to 0.64, at which important changes in the moments have occurred, leads to extensive supersonic flow over the forward half of the airfoil followed by well-established compression shock. These changes in both the lift and lift distribution over the airfoil lead to the effects on the peak moment coefficient shown in figure 5(e).

The data for the thick airfoils (figs. 5(a), 5(c), and 5(e)) indicate that the critical Mach number can be exceeded by an appreciable margin before important changes occur in the variation of moment coefficient with Mach number. This effect is believed to be a result of the local character of the supersonic field, which exists only in the immediate vicinity of the airfoil and extends over only a small chordwise portion of the airfoil. The same phenomenon is exhibited for the thinner airfoil (fig. 7(a)) but the value of critical Mach number is higher, as discussed under "Subcritical region."

In the negative stall region, changes of the order of 0.05 have taken place in the variation of moment coefficient with Mach number but these changes, except for the NACA 16-715 airfoil, have not been abrupt. The absence of abrupt changes is also indicated by the data of figure 7, which show that there are no decided changes in shape of the pressure-distribution diagrams within the Mach number range investigated. Calculation of the critical speed from theoretical pressure distribution would indicate that serious compression shock and therefore important flow changes might be expected at the highest speeds for which data are shown. Actually, separation phenomena probably occur which effectively delay the onset of compression shock. At speeds higher than the range of this investigation, abrupt changes might be expected.

The compressibility phenomena just discussed are believed to be common, at least qualitatively, to all airfoils in current use because in the stall region all airfoils exhibit a characteristic pressure peak near the leading edge and, hence, qualitatively have the same type of flow pattern. The present results indicate the effects of compressibility on these types of flow pattern.

Effects of Thickness on Peak Moment Coefficient

The variation of peak moment coefficient with thickness is shown in figure 8 for the NACA 16-209 and 16-215 airfoils. The results for the airfoils cambered to give lift coefficients of 0.5 and 0.7 at an angle of attack of 0° show the same type of variation and differ only in magnitude from the results presented in figure 8. The lines connecting the plotted points do not necessarily represent the variation between the points but serve in this case only to identify points at corresponding values of Mach number. These results show that an increase in thickness gives a numerical increase in the moment in both the positive and negative stall regions.

Another effect of increasing thickness is to accentuate the compressibility effects on the moment coefficient. This result is due to the greatest superstream velocities associated with greater thickness, as noted in the following discussion (fig. 7). This effect is illustrated by the different rates of change with thickness of the moment coefficients at low and high values of Mach number (fig. 8).

The changes in pressure distribution over the leading edge in the regions of stall are the underlying causes for the increases of peak moment coefficient with thickness. These changes are illustrated in figure 7. Theoretical considerations indicate a characteristic region of very high superstream velocities over the leading edge. The pressure distributions for the NACA 16-509 airfoil show a large reduction in the pressure peak over the leading edge as the angle is changed from -4° to -6° and indicate separation. It should be noted that this separation corresponds to the point at which the peak value of moment coefficient is attained. For the NACA 16-515 airfoil, however, such flow changes do not occur until beyond an angle of attack of -10°, so that higher moments occur owing to loading differences as a consequence of differences in the angle of attack of the two airfoils. The earlier reduction of the superstream velocities shown for the thinner sections is ascribed to their relatively sharper leading edges, as discussed under "Subcritical region." The changes noted here effect changes in the lift and moment of the airfoil. The pressure distributions presented in figure 7 were taken in the negative stall region; however, the same fundamental changes occur in the positive stall region.

Effects of Camber on Peak Moment Coefficient

The effects of increased camber on the peak moment coefficient (fig. 9) are, in the region of positive stall and for the range of Mach number tested, of the same magnitude as the effects associated with increased thickness (fig. 8). The variation of the moment coefficient about the quarter-chord axis with camber is, however, in the opposite direction from the variation with thickness. This result is ascribed to the change in distribution of the pressure load over the whole airfoil effected by camber, whereas the changes effected by thickness variation are principally changes in the loading over the forward portion of the airfoil due to change of nose radius (figs. 7 and 10).

The effects of camber variations on the moment coefficient in the negative stall region are smaller than those due to thickness variation, and the variation of the moment coefficient taken about the center-of-gravity axis is in the opposite direction. The variation of peak moment coefficient with camber appears to be little affected by increase of Mach number within the range investigated.

CONCLUSIONS

From an investigation of the compressibility effects on the peak section pitching-moment coefficients of six NACA 16-series airfoils, the following conclusions have been made:

1. The peak pitching-moment coefficients, which were encountered in the regions of positive and negative stall, underwent important changes due to compressibility effects. In several instances, variations of pitching-moment coefficient of 0.025 to 0.10 were encountered for the thicker and more highly cambered airfoils tested.

2. Critical speeds as low as a Mach number of 0.30 were encountered and marked changes of peak pitching-moment coefficient occurred at Mach numbers as low as 0.53.

3. Extrapolation of low-speed data according to the Glauert-Ackeret relation $1/\sqrt{1 - M^2}$ gave valid or conservative estimates of the variation with Mach number

in the subcritical region. Because of the low critical speeds associated with operation in the stall region, however, this method is limited in application.

4. Increasing the thickness and camber of an airfoil in compressible flow accentuated the compressibility effects on the aerodynamic pitching moment. An increase in the value of the pitching-moment coefficient was found to occur with an increase in thickness.

Langley Memorial Aeronautical Laboratory
National Advisory Committee for Aeronautics
Langley Field, Va.

REFERENCES

1. Stack, John: The N.A.C.A. High-Speed Wind Tunnel and Tests of Six Propeller Sections. NACA Rep. No. 463, 1933.

2. Stack, John, and von Doenhoff, Albert E.: Tests of 16 Related Airfoils at High Speeds. NACA Rep. No. 492, 1934.

3. Stack, John, Lindsey, W. F., and Littell, Robert E.: The Compressibility Burble and the Effect of Compressibility on Pressures and Forces Acting on an Airfoil. NACA Rep. No. 646, 1938.

4. Stack, John: Tests of Airfoils Designed to Delay the Compressibility Burble. NACA TN No. 976, Dec. 1944. (Reprint of ACR, June 1939.)

5. Vincenti, Walter G., and Graham, Donald J.: The Effect of Wall Interference upon the Aerodynamic Characteristics of an Airfoil Spanning a Closed-Throat Circular Wind Tunnel. NACA ACR No. 5D21, 1945.

TABLE I

ANGLES OF ATTACK AND MACH NUMBERS AT WHICH
PEAK LIFT AND MOMENT COEFFICIENTS OCCUR

Mach number	Angle of attack (deg)											
	Positive stall			Negative stall			Positive stall			Negative stall		
	$c_{l_{max}}$	$c_{m_{c/4}}$	$c_{m_{c.g.}}$	c_l	$c_{m_{c/4}}$	$c_{m_{c.g.}}$	$c_{l_{max}}$	$c_{m_{c/4}}$	$c_{m_{c.g.}}$	c_l	$c_{m_{c/4}}$	$c_{m_{c.g.}}$
	NACA 16-209 airfoil						NACA 16-215 airfoil					
0.12	10	8	9	-9	-6	-8	-----	-----	------	-14	-11	-11
.20	10	9	8	-10	-6	-8	13	13	13	-11	-11	-11
.25	10	8	9	-8	-6	-7	14	14	14	-11	-11	-11
.33	10	8	8	-10	-6	-8	12	13	13	-11	-11	-11
.40	10	8	8	-10	-6	-8	11	12	11	-12	-10	-10
.48	10	8	8	-10	-6	-7	11	11	11	-11	-11	-11
.53	9	6	8	-8	-6	-7	10	11	10	-11	-10	-11
.57	-----	-----	------	-10	-6	-7	-----	-----	------	---	-----	------
.60	-----	-----	------	-10	-6	-7	10	10	10	-11	-10	-10
.64	-----	-----	------	---	-----	------	8	11	9	---	-----	------
	NACA 16-509 airfoil						NACA 16-515 airfoil					
0.12	10	10	10	-8	-6	-6	14	15	14	-9	-9	-9
.20	10	10	10	-8	-6	-6	15	16	16	-9	-10	-9
.25	9	10	10	-14	-6	-8	14	16	14	-10	-10	-10
.33	10	10	10	-10	-6	-6	14	15	15	-9	-10	-10
.40	9	10	8	-12	-6	-7	12	12	12	-10	-9	-9
.48	8	8	8	-10	-6	-8	12	12	12	-9	-9	-9
.53	8	8	8	-10	-6	-6	12	11	11	-8	-8	-8
.60	-----	-----	------	-10	-4	-6	-----	-----	------	-10	-8	-8
.64	-----	-----	------	-10	-6	-6	-----	-----	------	-7	-8	-8
.68	-----	-----	------	---	-6	-6	-----	-----	------	---	-----	------
	NACA 16-709 airfoil						NACA 16-715 airfoil					
0.12	11	10	10	---	-----	------	14	16	15	-12	-6	-8
.20	9	10	10	-8	-5	-7	14	16	15	-9	-8	-9
.25	10	10	10	-8	-5	-6	14	14	14	-10	-10	-10
.33	10	10	10	-8	-4	-6	16	14	15	-8	-8	-8
.40	10	10	10	-8	-4	-6	14	14	14	-8	-8	-8
.48	9	10	9	-8	-4	-5	14	14	14	-10	-8	-9
.53	9	9	9	-8	-4	-6	14	12	13	-10	-10	-10
.60	9	9	9	-8	-5	-6	10	10	10	-7	-8	-9
.64	-----	-----	------	-8	-4	-6	8	11	12	-10	-9	-8

NATIONAL ADVISORY
COMMITTEE FOR AERONAUTICS

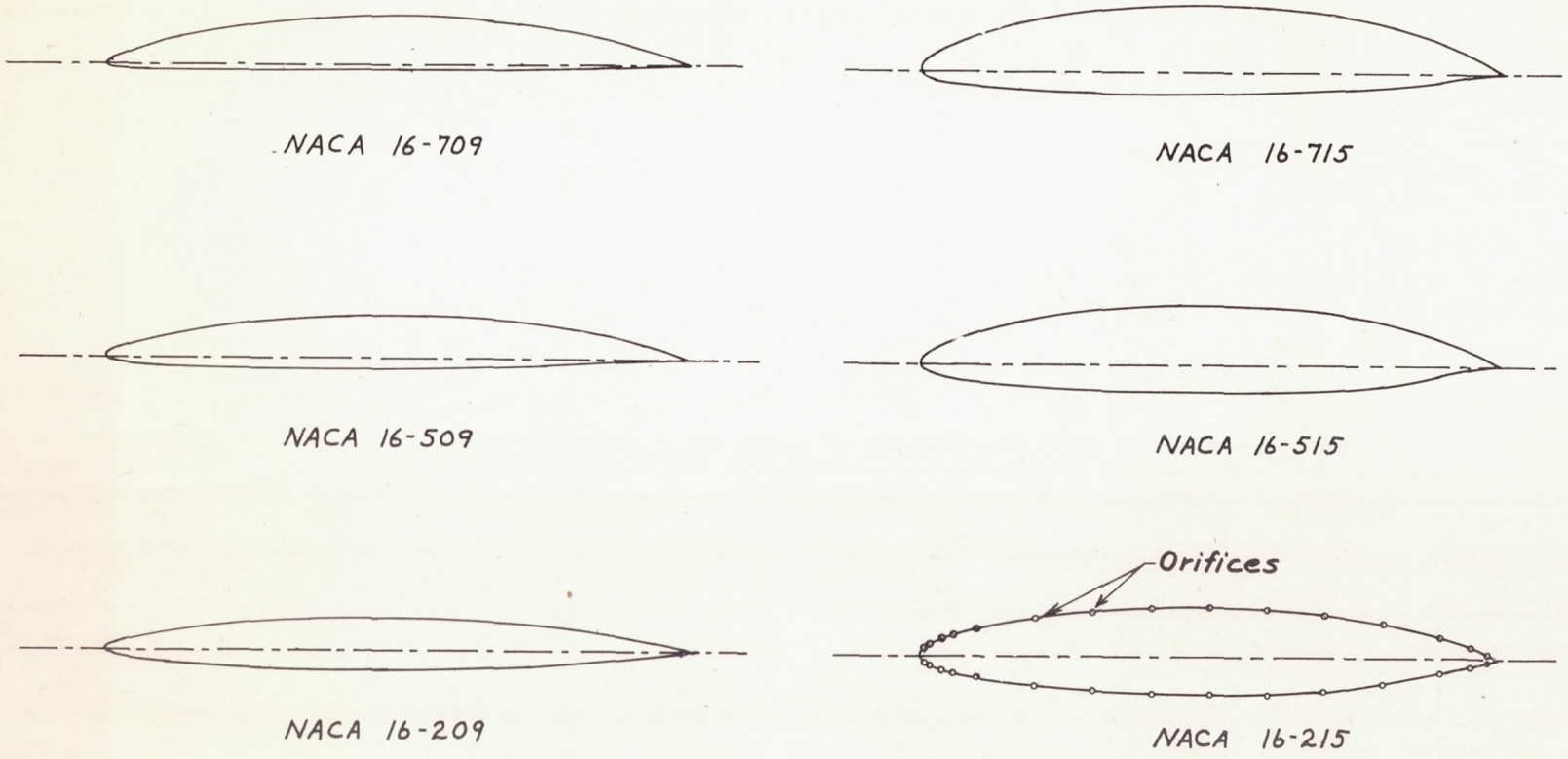

Figure 1.- Airfoil profiles tested and distribution of pressure orifices.

L-515

NATIONAL ADVISORY
COMMITTEE FOR AERONAUTICS

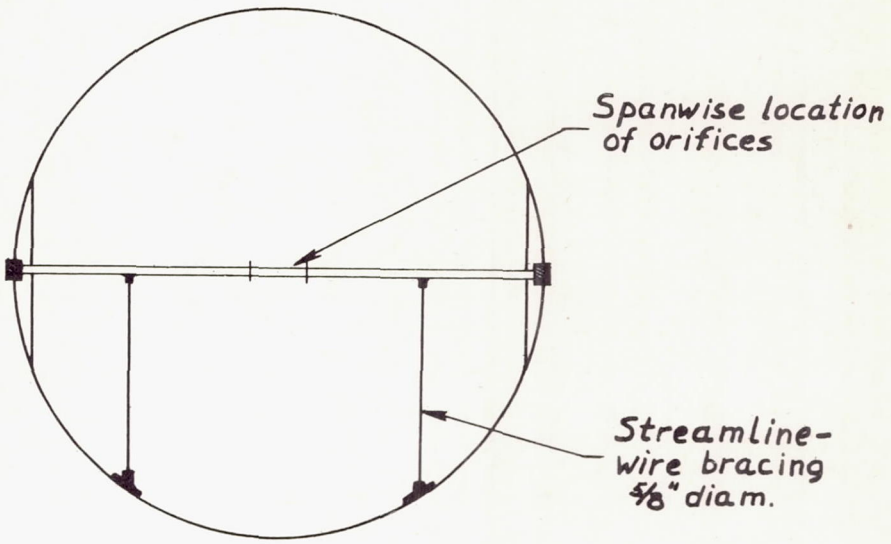

(a) Airfoil mounting in tunnel.

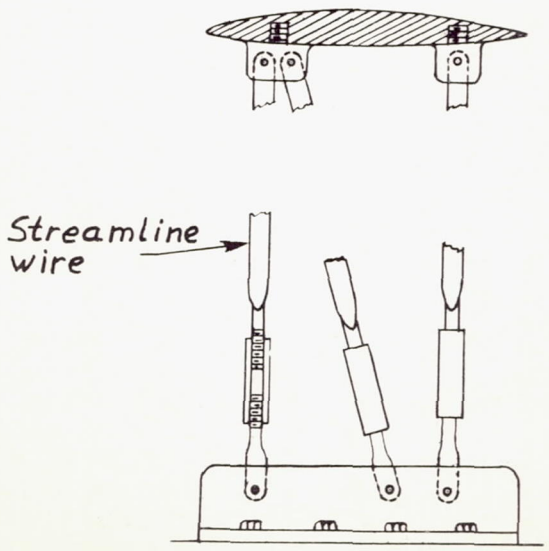

(b) Detail of bracing.

Figure 2.- Diagrammatic sketch of airfoil mounting and bracing in the NACA 8-foot high-speed tunnel.

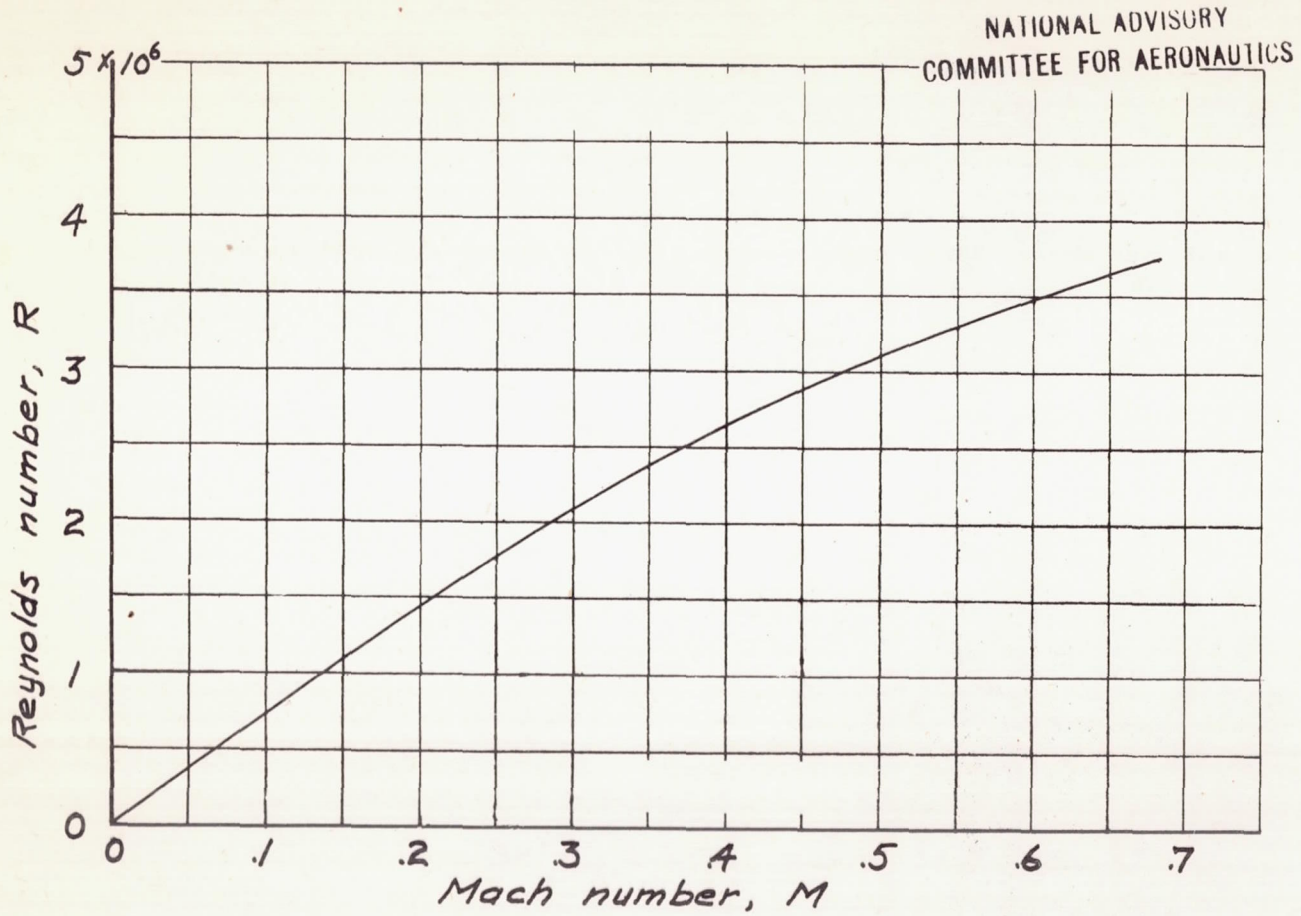

Figure 3.- Variation of Reynolds number with Mach number for 1-foot-chord airfoils in the NACA 8-foot high-speed tunnel.

L-515

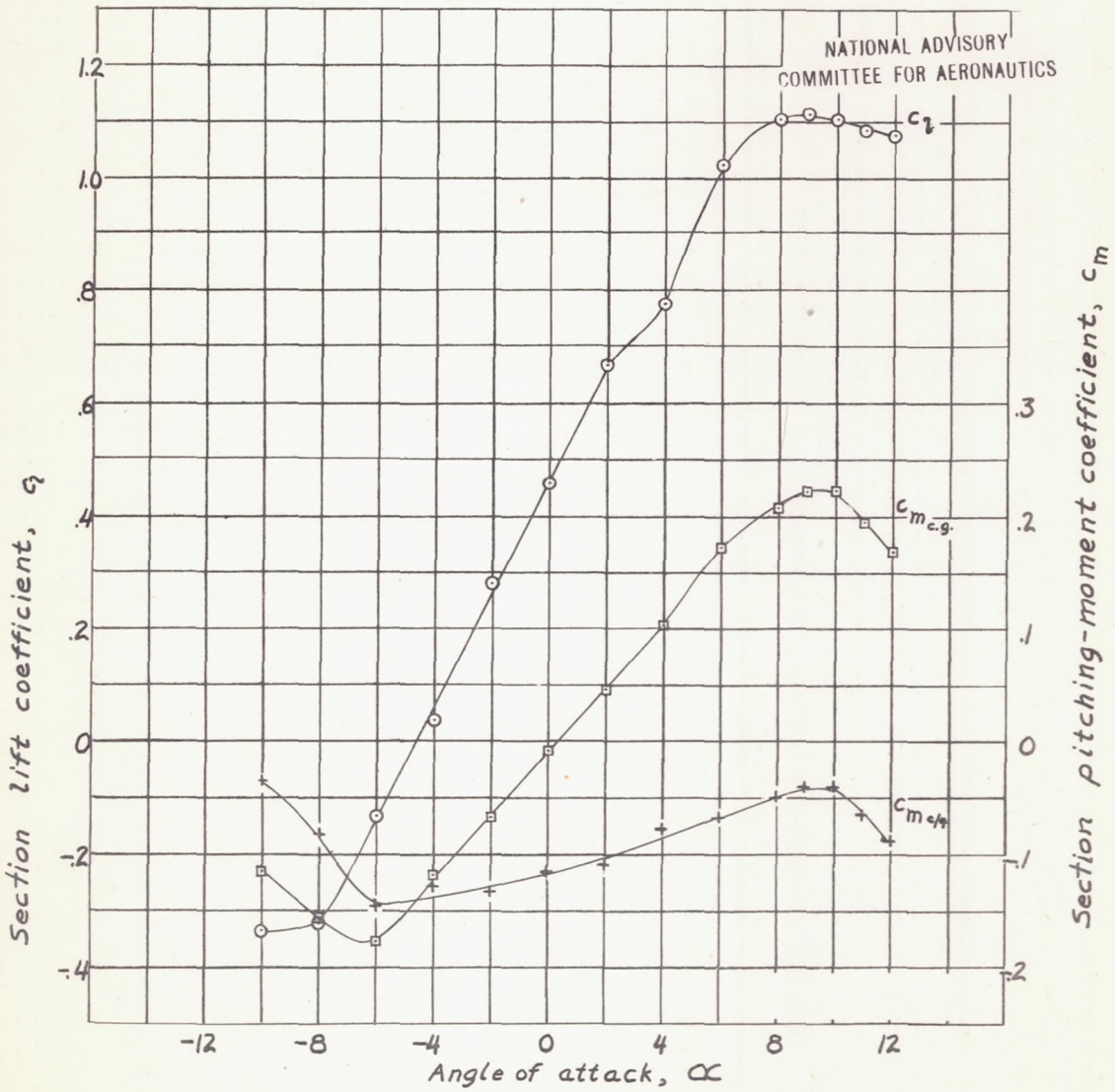

Figure 4.- Variation of section lift and pitching-moment coefficients with angle of attack for the NACA 16-509 airfoil at a Mach number of 0.33.

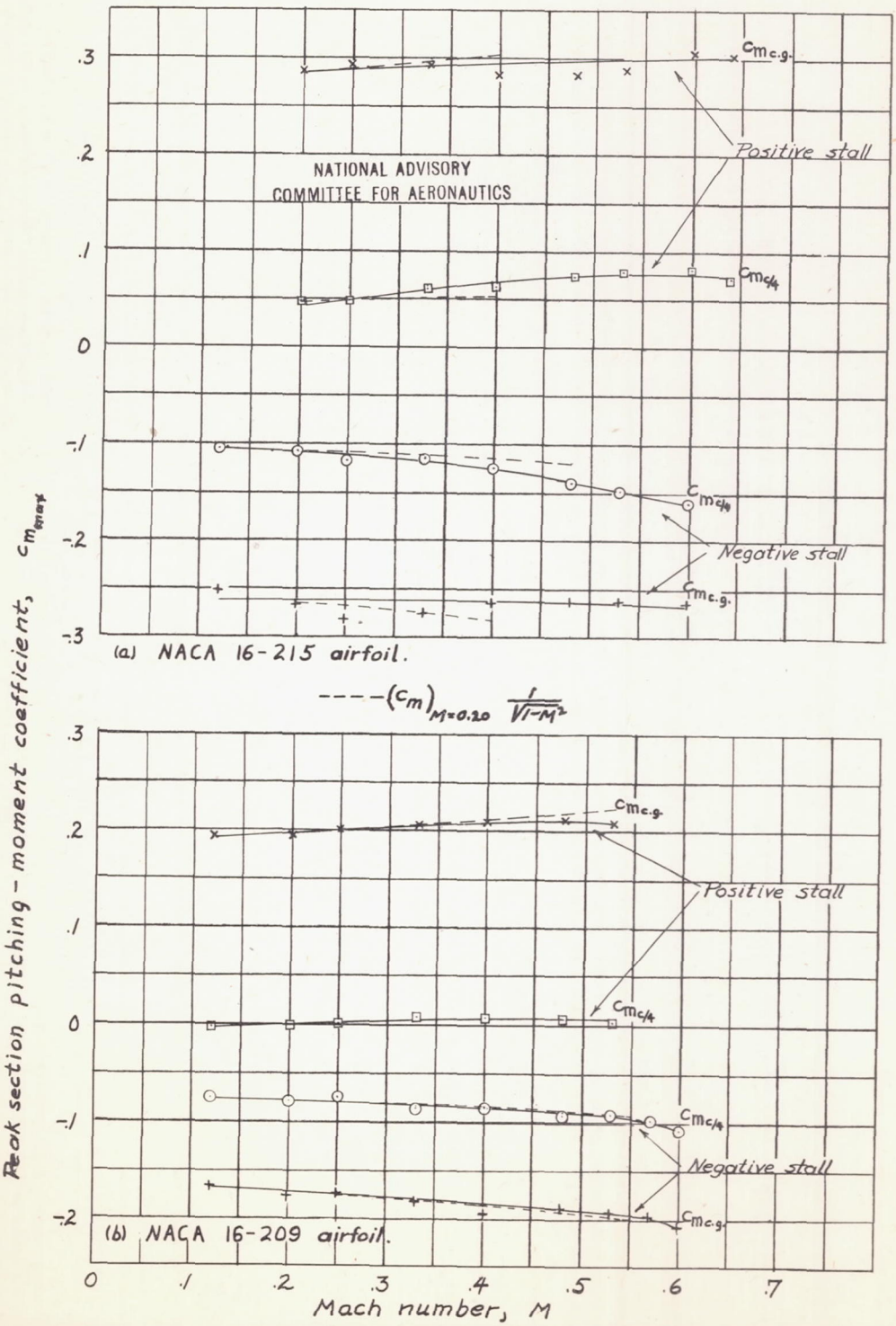

Figure 5.— Variation of peak positive and negative pitching-moment coefficients with Mach number for six 1-foot-chord NACA 16-series airfoils.

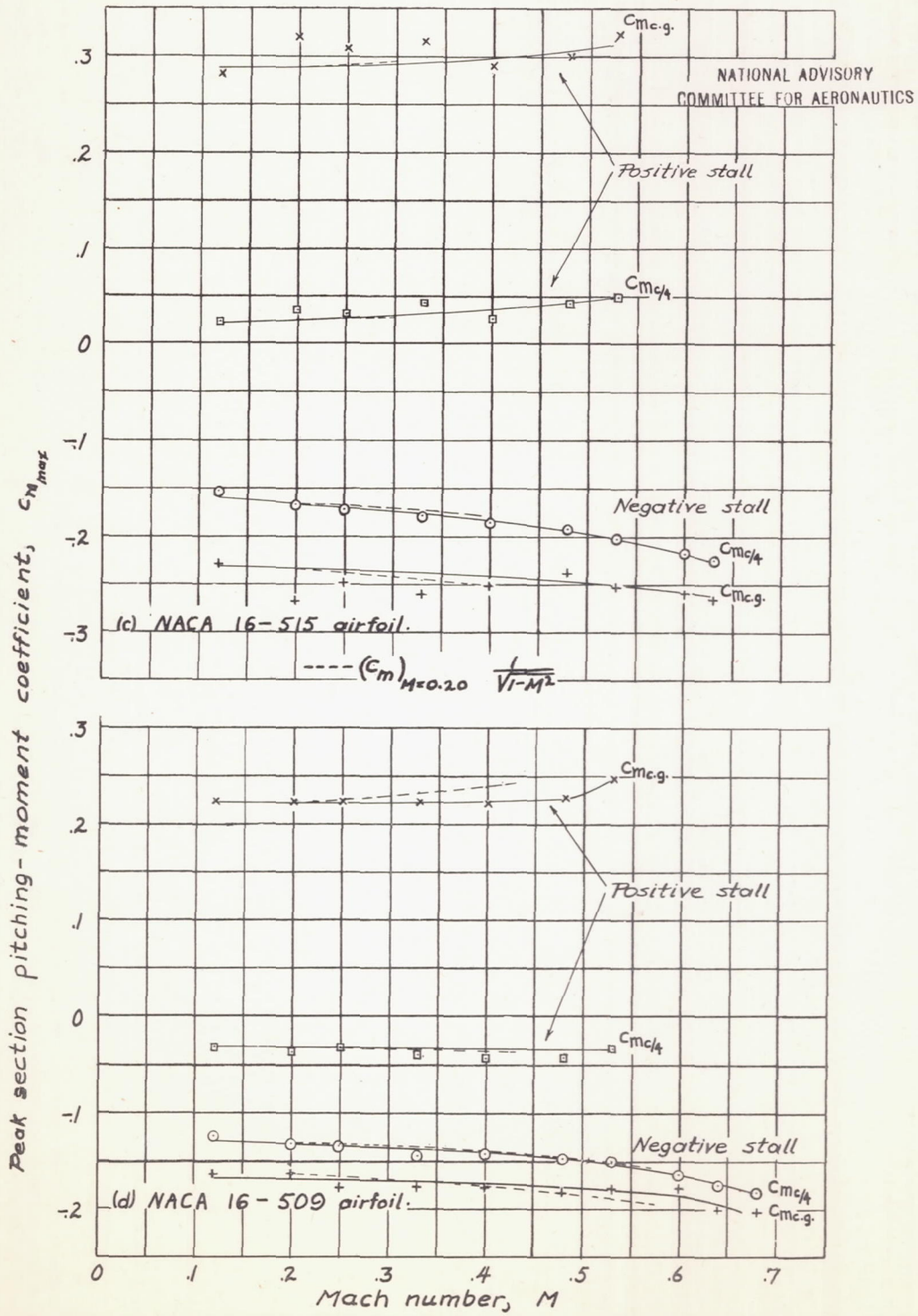

Figure 5.- Continued.

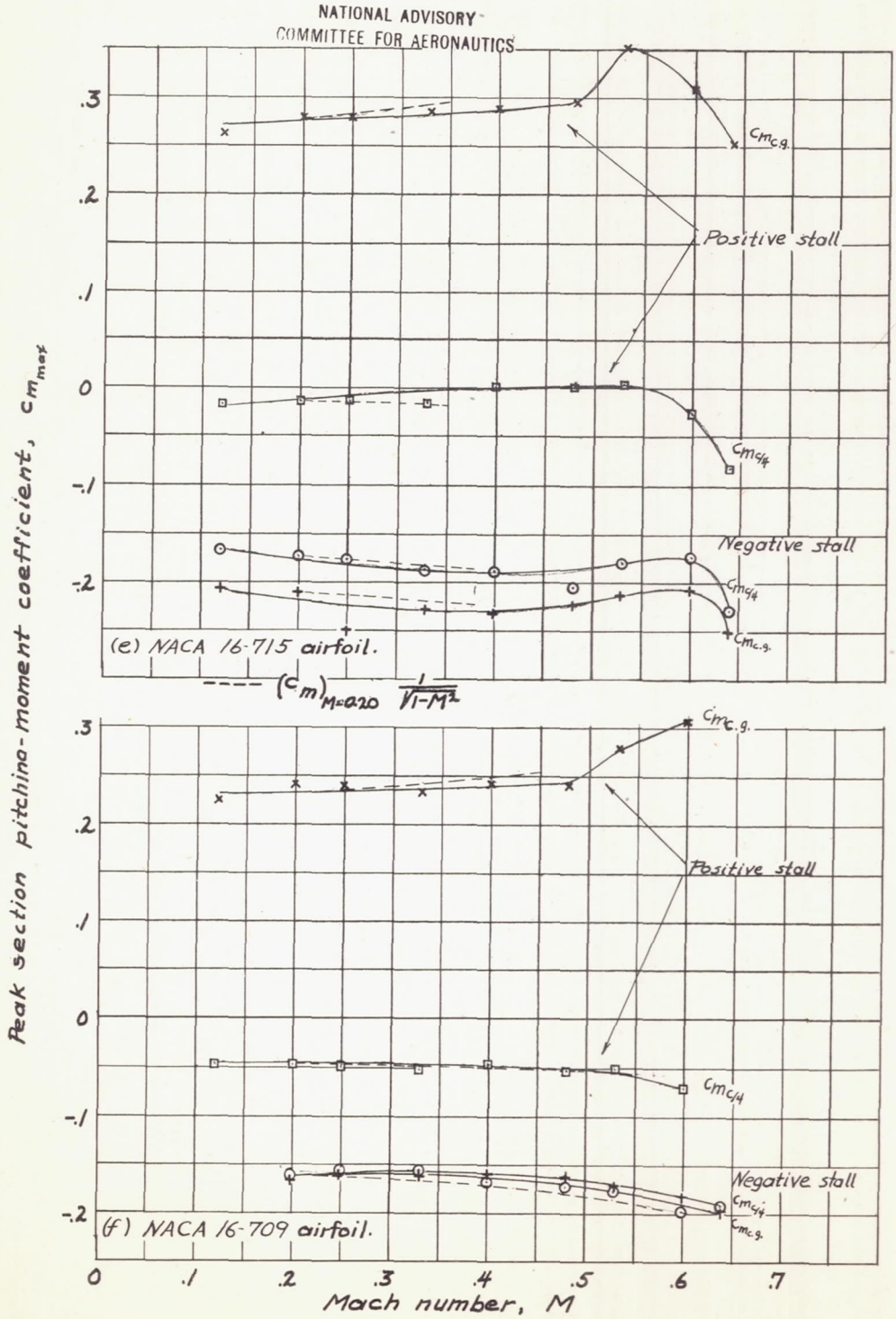

Figure 5.- Concluded.

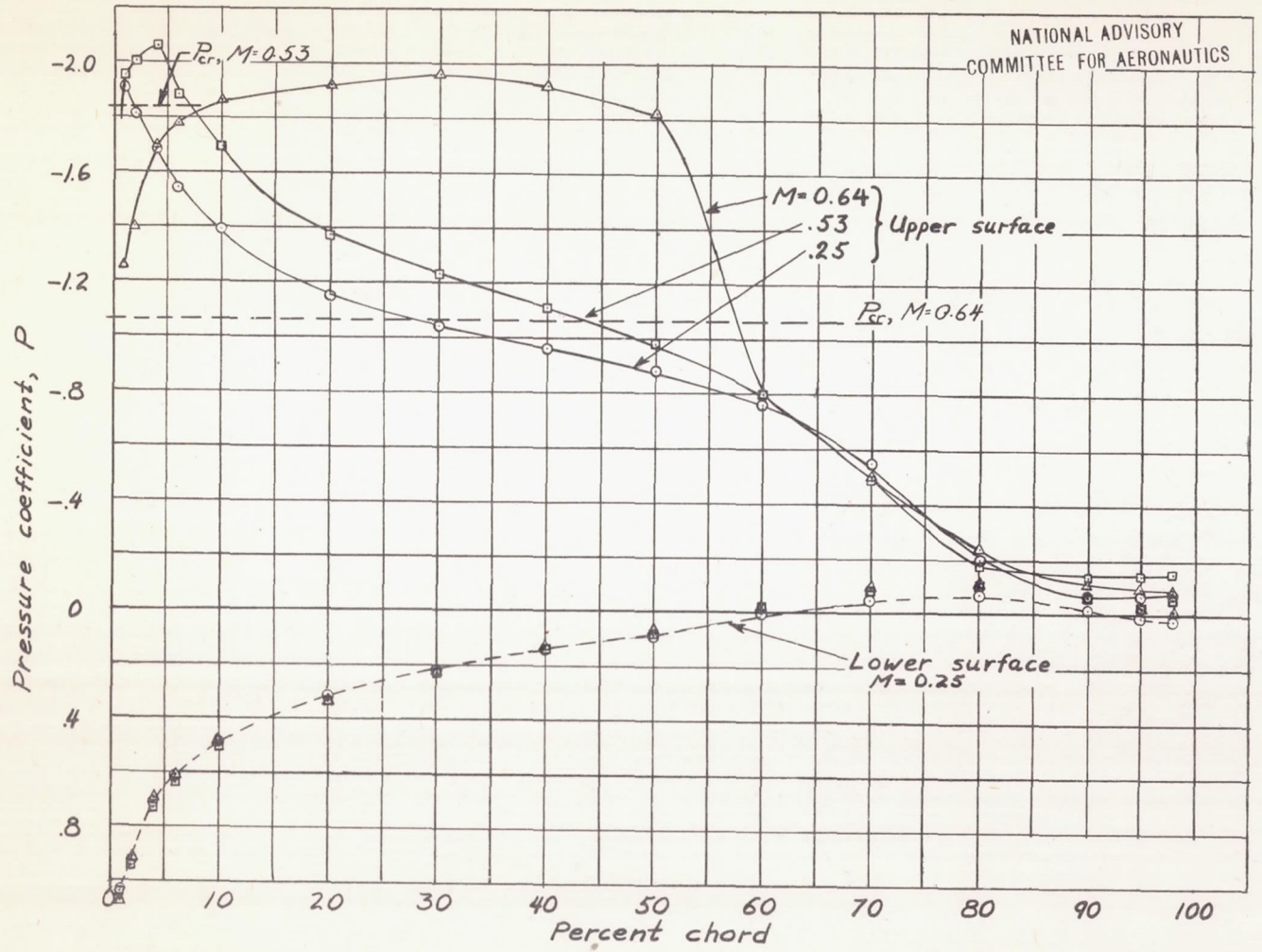

Figure 6 .- Pressure distribution over the NACA 16-715 airfoil at an angle of attack of 8° for three values of Mach number.

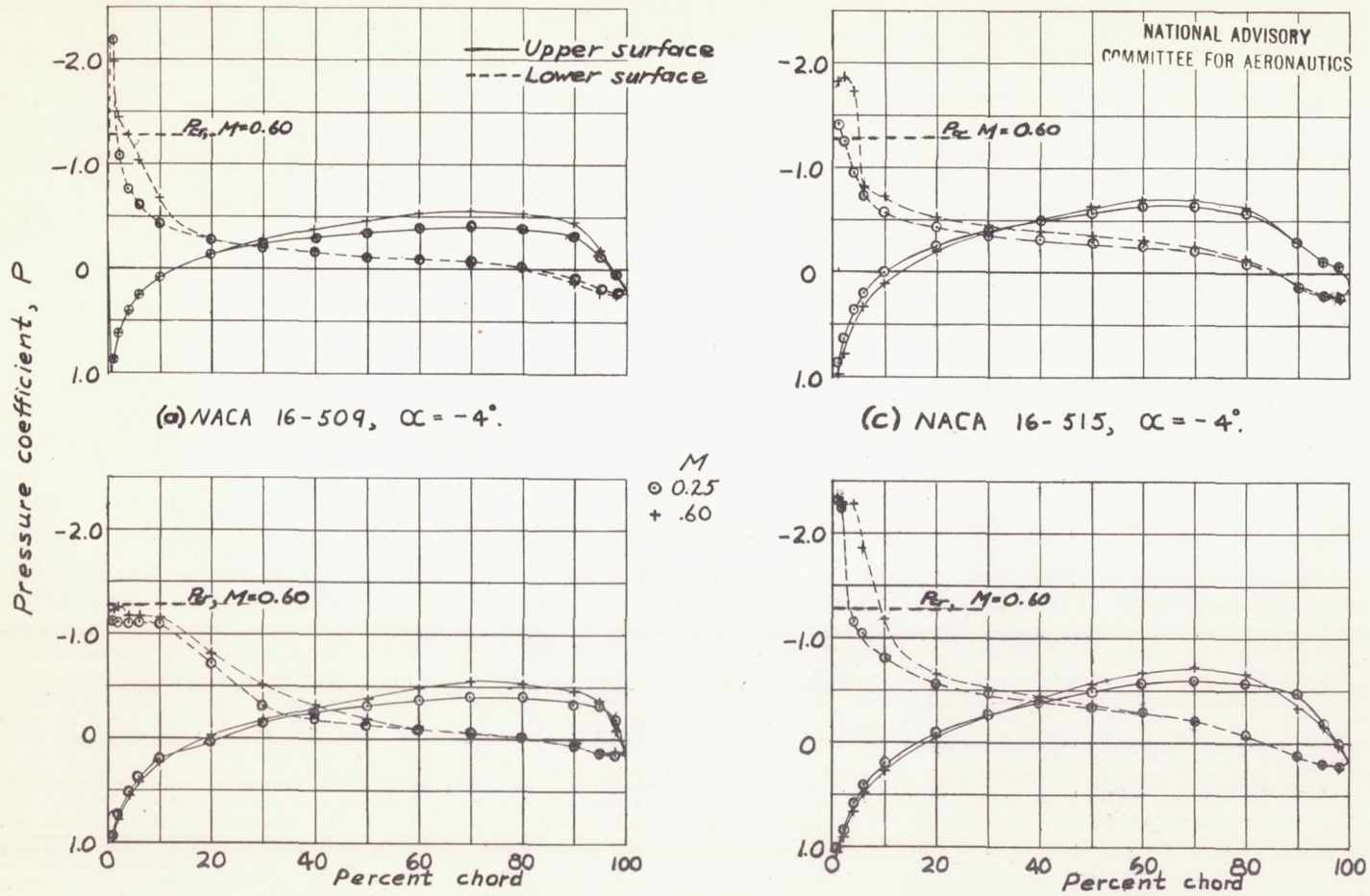

(a) NACA 16-509, $\alpha = -4°$.

(c) NACA 16-515, $\alpha = -4°$.

(b) NACA 16-509, $\alpha = -6°$.

(d) NACA 16-515, $\alpha = -6°$.

Figure 7.- Comparison of pressure distributions over 1-foot-chord NACA 16-509 and 16-515 airfoils at four negative angles of attack at M = 0.25 and M = 0.60.

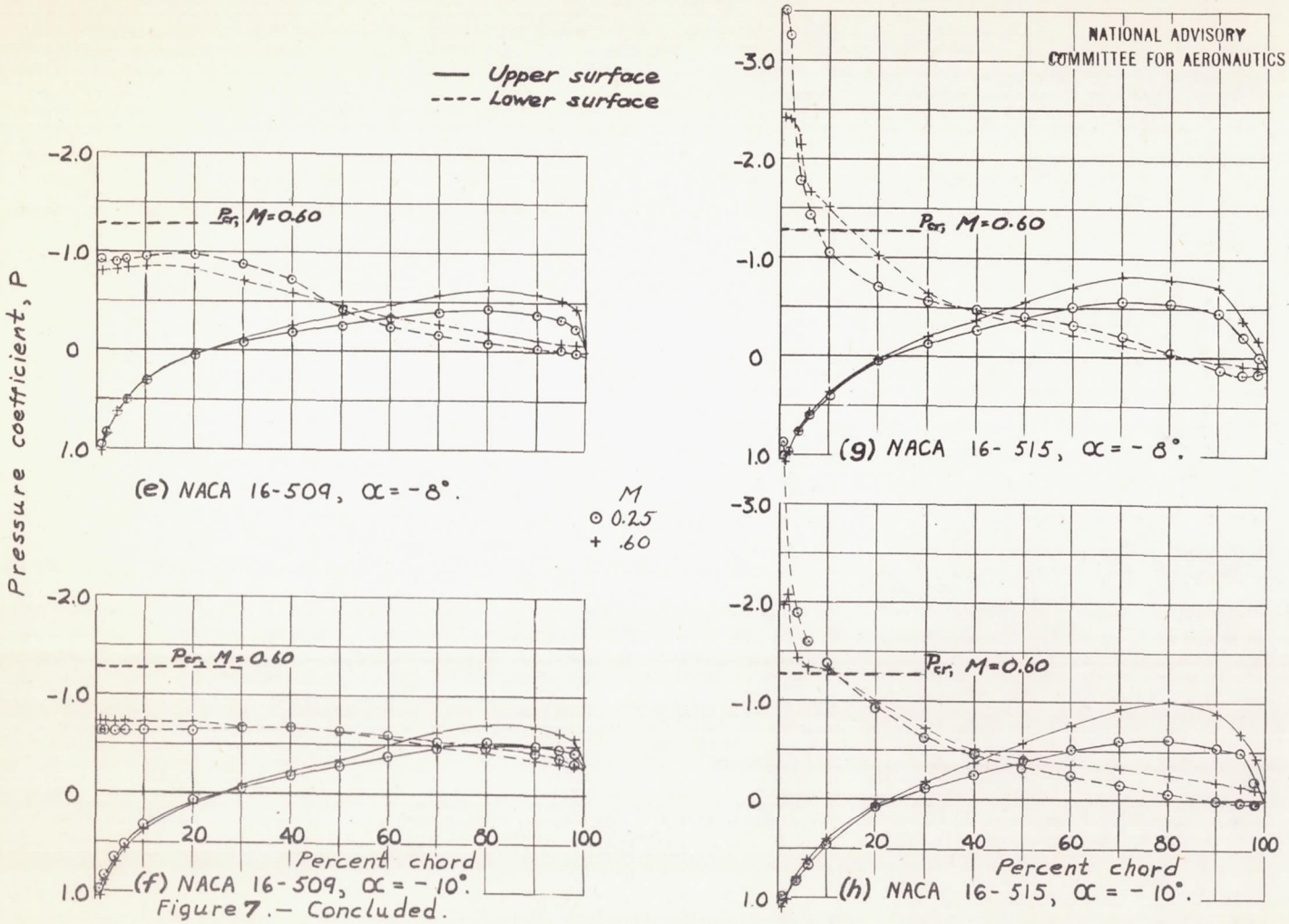

Figure 7.- Concluded.

L-515

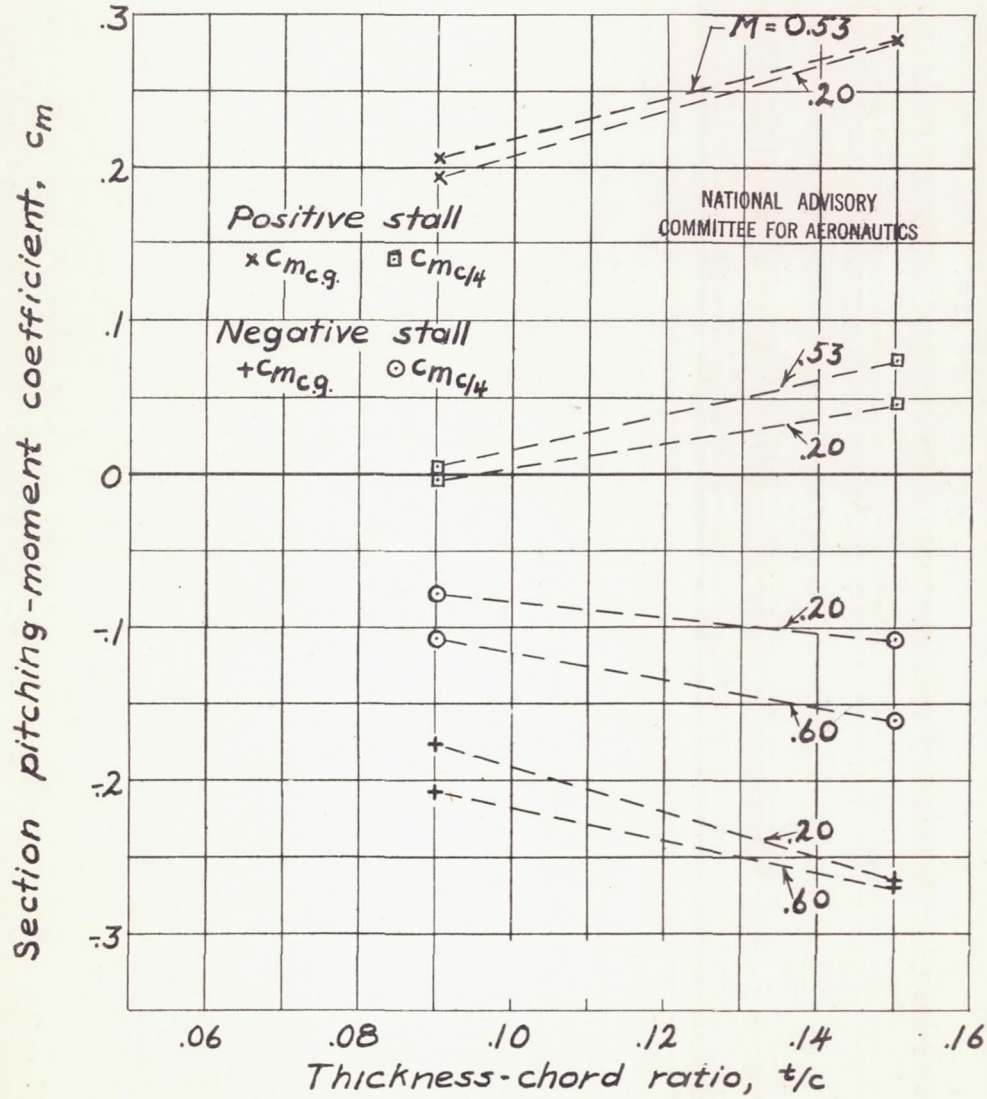

Figure 8.– Variation of peak positive and negative pitching-moment coefficients with thickness-chord ratio for NACA 16-series airfoils with camber designed to give $c_l = 0.2$ at an angle of attack of 0°.

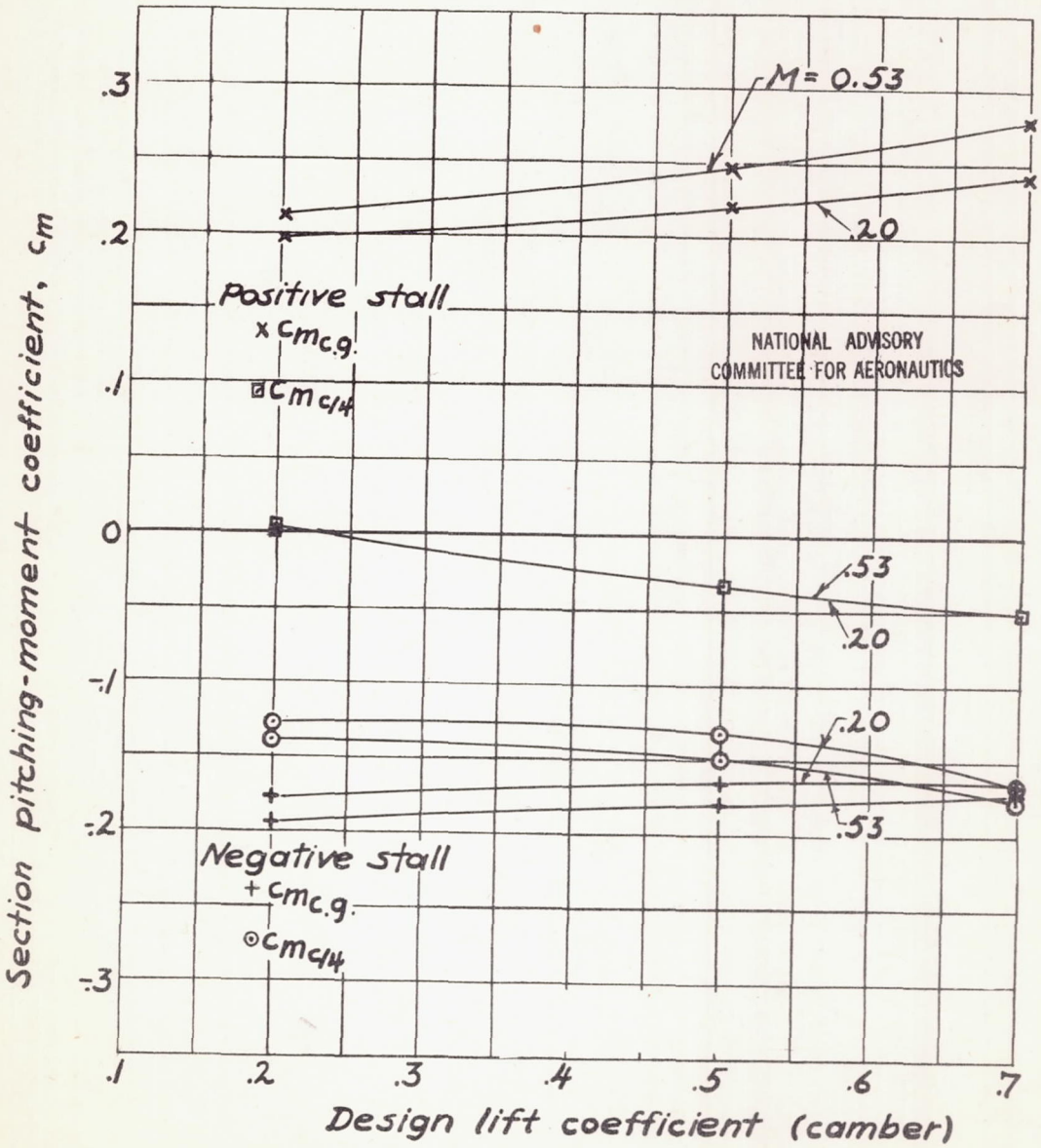

(a) t/c = 0.09.

Figure 9.- Variation of peak positive and negative pitching-moment coefficients with design lift coefficient for NACA 16-series airfoils.

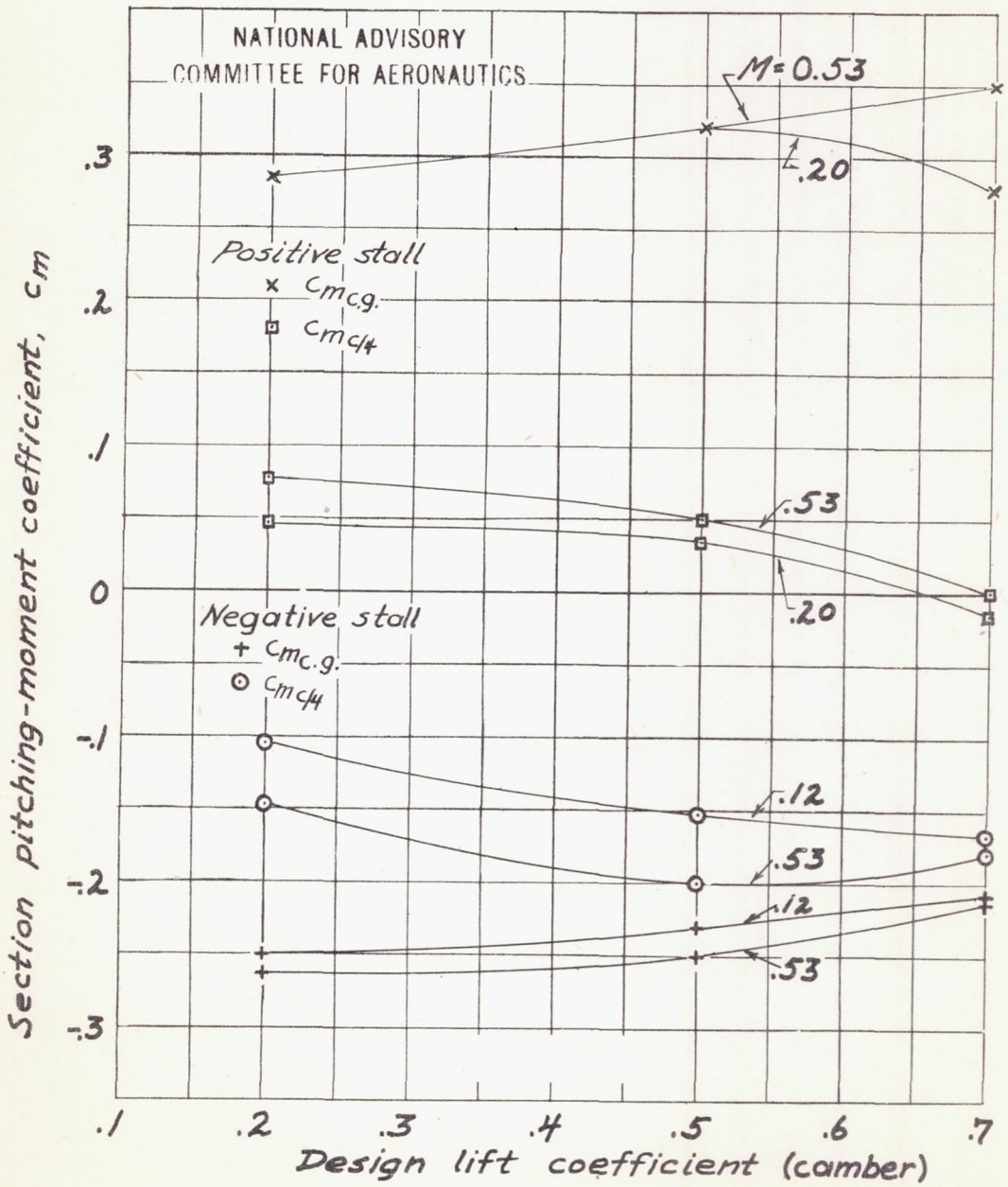

(b) $t/c = 0.15$.

Figure 9.- Concluded.

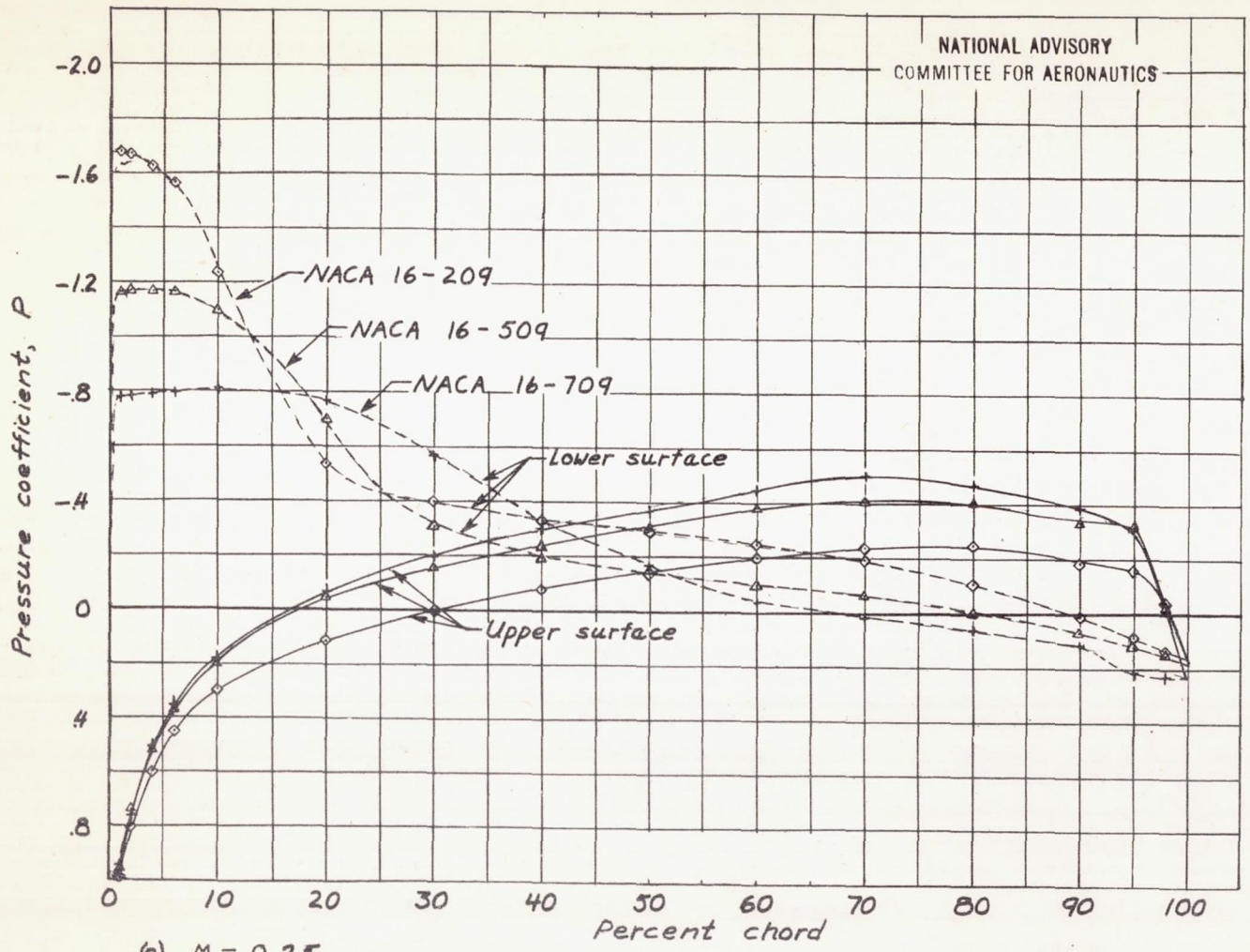

(a) M = 0.25.

Figure 10.— Pressure distributions over three 1-foot-chord NACA 16-series airfoils at $\alpha = -6°$.

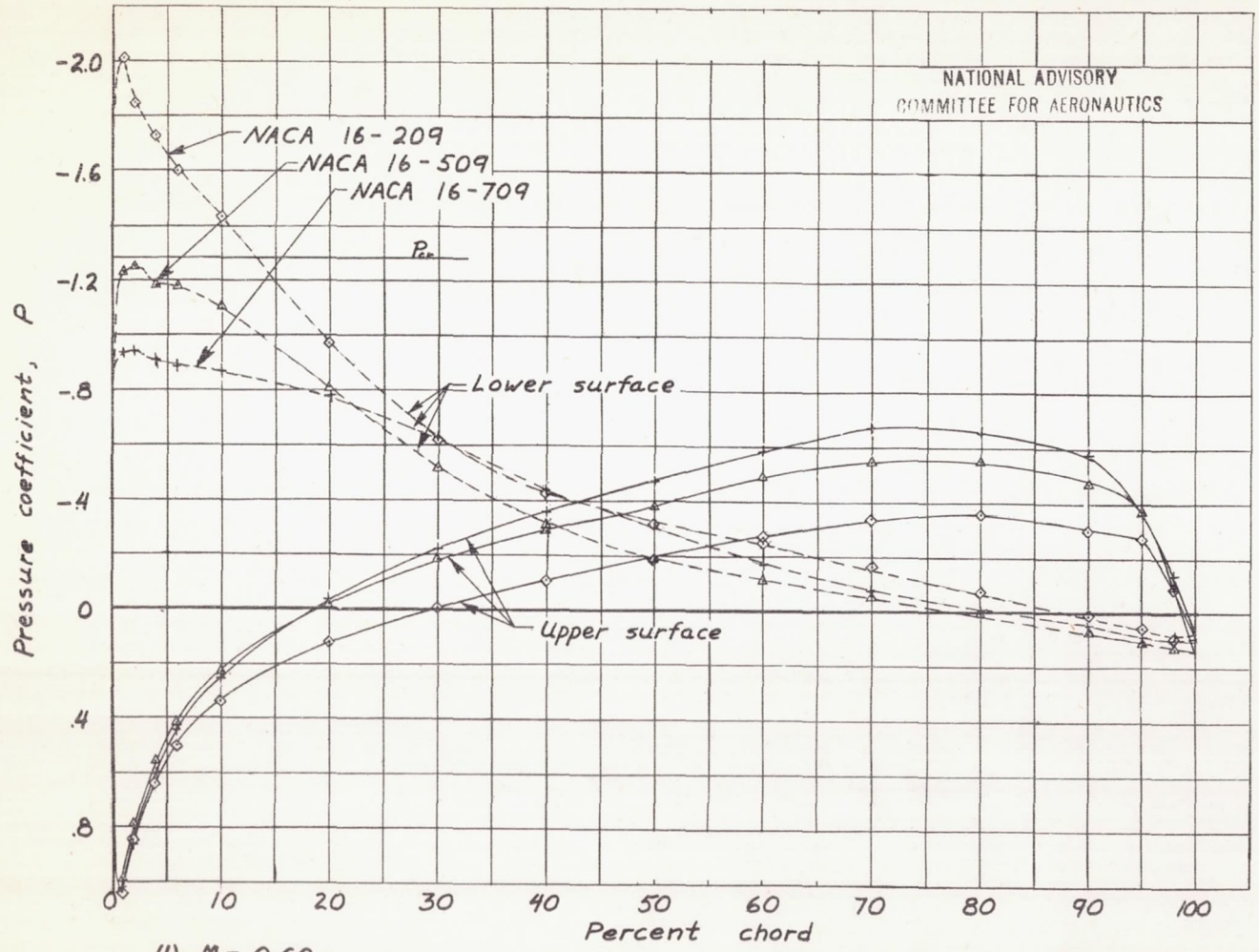

(b) M = 0.60.

Figure 10.— Concluded.